

5-Demethylnobiletin and 5-Acetoxy-6,7,8,3',4'-pentamethoxyflavone Suppress Lipid Accumulation by Activating the LKB1-AMPK Pathway in 3T3-L1 Preadipocytes and High Fat Diet-Fed C57BL/6 Mice

Yen-Chen Tung,^{†,§} Shiming Li,[#] Qingrong Huang,[†] Wei-Lun Hung,[†] Chi-Tang Ho,[†] Guor-Jien Wei,^{*,⊗} and Min-Hsiung Pan^{*,#,§,⊠,Δ}

[†]Department of Food Science, Rutgers University, New Brunswick, New Jersey 08901, United States

[§]Institute of Food Sciences and Technology, National Taiwan University, Taipei 106, Taiwan

[#]Hubei Key Laboratory of Economic Forest Germplasm Improvement and Resources Comprehensive Utilization and Hubei Collaborative Innovation Center for the Characteristic Resources Exploitation of Dabie Mountains, Huanggang Normal University, Huanggang, Hubei China

[⊗]Department of Nutrition and Health Sciences, Kainan University, Taoyuan 33857, Taiwan

[⊠]Department of Medical Research, China Medical University Hospital, China Medical University, Taichung, Taiwan

^ΔDepartment of Health and Nutrition Biotechnology, Asia University, Taichung, Taiwan

Supporting Information

ABSTRACT: Polymethoxyflavones (PMFs) and hydroxylated polymethoxyflavones (HPMFs), such as nobiletin (Nob) and 5-demethylnobiletin (5-OH-Nob), are unique flavonoids that are found exclusively in citrus peels. Nobiletin has been shown to suppress adipogenesis *in vitro*, but the antiadipogenic activity of 5-OH-Nob has not been investigated. Both nobiletin and 5-OH-Nob have poor aqueous solubility and low oral bioavailability. We employed chemical modification to produce the acetyl derivative of 5-OH-Nob, that is, 5-acetyloxy-6,7,8,3',4'-pentamethoxyflavone (5-Ac-Nob), to improve its bioavailability and bioactive efficiency. We found that 5-Ac-Nob reduced triacylglycerol (TG) content to a greater extent than 5-OH-Nob in 3T3-L1 preadipocytes. Orally administered 5-Ac-Nob resulted in a significant reduction in body weight, intra-abdominal fat, plasma and liver TG levels, and plasma cholesterol level in high fat diet-induced obese male C57BL/6J mice. The 5-Ac-Nob treatment decreased lipid accumulation by triggering the adenosine 5'-monophosphate-activated protein kinase (AMPK) pathway to alter transcriptional factors or lipogenesis-related enzymes *in vivo* and *in vitro*.

KEYWORDS: 5-acetyloxy-6,7,8,3',4'-pentamethoxyflavone, high-fat diet, 3T3-L1 preadipocytes, LKB1-AMPK pathway

INTRODUCTION

In 2015, the World Health Organization estimated that >1.9 billion adults are overweight and >600 million people are obese.¹ An energy imbalance is the major cause of obesity. During adipogenesis, excess calories are stored as triacylglycerols (TGs), and the number and size of adipocytes are increased. In lipogenesis, the syntheses of fatty acids and TGs occurs in the liver and adipose tissues, which eventually expands the adipose tissues.^{2,3} The function of brown adipose tissues is different from that of white adipose tissues (WAT) in the body. WAT is not only a major TG storage tissue that can be deposited under the skin and in the intra-abdominal area but also an endocrine organ that regulates whole-body energy homeostasis. When there is a positive energy balance, adipose tissue dysfunction may develop, and ectopic fat, especially intra-abdominal fat, will be deposited in several organs, such as the liver, pancreas, and heart, affecting their functions.^{2,4} Therefore, obesity plays a key role in metabolic syndromes and is strongly associated with diabetes, cardiovascular disease, fatty liver disease, and cancer.^{4,5} Transcription factors play a crucial role in controlling glucose, amino acid, and lipid metabolic homeostasis. Sterol regulatory element-binding protein-1 (SREBP-1) is an important transcription factor involved in cellular lipogenesis, lipid homeostasis, and adipocyte

differentiation.^{4,6,7} In addition, AMPK is a major regulator of cellular energy balance that switches on the catabolic pathway and switches off the anabolic pathway.⁸ AMPK can regulate several metabolic pathways, including glucose transport, gluconeogenesis, lipogenesis, and lipolysis.⁹ AMPK can control lipid metabolism by phosphorylating acetyl-CoA carboxylases (ACC) 1 and 2 or regulating the long-term effects of phosphorylated SREBP-1 and the loss of expression of lipogenic enzymes.¹⁰

Polymethoxyflavones (PMFs) and hydroxylated polymethoxyflavones (HPMFs) are flavonoids found in citrus peels. They have several biological benefits, such as anti-inflammatory and anticancer activities and regulation of lipid metabolism.¹¹ Nobiletin (Nob) and HPMFs can suppress lipid accumulation in 3T3-L1 preadipocytes and high-fat diet-induced obese animal models,^{12,13} but the antiadipogenic effects of 5-demethylnobiletin (5-OH-Nob) are still unknown. It has been reported that both PMFs and HPMFs are highly lipophilic and have poor aqueous solubility and low oral bioavailability.¹⁴ Prodrugs are derivatives of

Received: February 12, 2016

Revised: April 2, 2016

Accepted: April 4, 2016

drug molecules. During metabolism, the active parent drugs derived from prodrugs will be released. The formulation of a prodrug can improve aqueous solubility, chemical stability, presystemic metabolism, and brain penetration.¹⁵ Chemical modification is one of the methods of prodrug formation.¹⁶ Recently, Wang et al. used chemical modification to obtain 5-acetyloxy-6,7,8,4'-tetramethoxyflavone (5-Ac-Tan), which had improved anti-breast cancer activity compared to tangeretin.¹⁷ In our current study, based on the prodrug concept, we prepared 5-OH-Nob and 5-acetyloxy-6,7,8,3',4'-pentamethoxyflavone (5-Ac-Nob) from nobletin by chemical modification, and their antiadipogenic activities in the 3T3-L1 preadipocytes and a high-fat diet-induced obese animal model, as well as the related molecular mechanisms, were investigated.

MATERIALS AND METHODS

Chemicals and Reagents. Powder of PMFs was obtained from BioGin Biochemicals Co., Ltd. (Chengdu, Sichuan, China). Methanol, ethanol, water, acetonitrile, chloroform, ethyl acetate, hexanes, 2-propanol, diethyl ether, and acetone were of HPLC grade and purchased from Fisher Scientific (Springfield, NJ, USA). Thin layer chromatography (TLC) plates were purchased from Analtech (Newark, DE, USA). Enhanced chemiluminescent-based detection system (ECL) and Hybond-polyvinylidene difluoride (PVDF) membrane were purchased from Millipore (Billerica, MA, USA). Acrylamide, prestained protein markers, dimethyl sulfoxide (DMSO), glycerol, and Tris-HCl were purchased from Merck (Whitehouse Station, NJ, USA). Bio-Rad protein assay reagent was purchased from Bio-Rad Laboratory (Hercules, CA, USA). Dulbecco's modified Eagle's medium (DMEM), penicillin-streptomycin, fetal calf serum (FCS), and fetal bovine serum (FBS) were purchased from Gibco BRL (Grand Island, NY, USA). Anti- β -actin antibody, insulin, 3-isobutylmethylxanthine (IBMX), dexamethasone (DEX), and isopropanol were purchased from Sigma Chemical Co. (St. Louis, MO, USA). Anti-phosphorylated AMPK (pAMPK α), anti-AMPK α , anti-LKB1, anti-phosphorylated LKB1 (pLKB1), and anti-fatty acid synthase (FAS) antibodies were purchased from Cell Signaling Technology (Beverly, MA, USA). Other antibodies used in this study were purchased from Santa Cruz Biotechnology (Santa Cruz, CA, USA).

Preparation of 5-OH-Nob and 5-Ac-Nob. PMF crude extracts were purified by silica gel column chromatography with a mixture of solvent (hexane/ethyl acetate = 4:1) eluents to obtain nobletin as a white powder. 5-OH-Nob was prepared by refluxing nobletin with concentrated HCl in 95% aqueous ethanol for 16 h, followed by concentration, acidification, extraction with ethyl acetate, and concentration again prior to another silica gel column chromatography yielding 5-OH-Nob with a minimum purity of 99%. By employing the same synthetic methodology described in a previous paper,¹⁷ the preparation of 5-Ac-Nob started with refluxing of 5-OH-Nob with acetic anhydride in methylene chloride with pyridine as a base overnight, then concentration and aqueous workup with ethyl acetate to yield a crude product after concentration in vacuo. The crude mixture from the reaction was subject to purification on a flash silica gel column with hexanes and ethyl acetate as eluting solvents to yield 5-Ac-Nob as a pale yellow solid with a purity score of $\geq 99\%$. NMR spectra were recorded on a Bruker AVIII 500 MHz FT-NMR (Bruker, Rheinstetten, Germany) in CDCl₃. LC-MS was performed by a Thermo Scientific linear ion trap mass spectrometer (LXQTM) in positive ionization mode (Thermo Scientific, Waltham, MA, USA). The results of NMR and LC-MS are also given in the Supporting Information. In MS positive mode, 5-OH-Nob and 5-Ac-Nob exhibited protonated molecules of [M + H]⁺ at *m/z* 389.28 and 431.08, respectively (Supplementary Figures 1 and 2). The proton NMR spectra of 5-OH-Nob was as follows: ¹H NMR (CDCl₃) δ 3.96 (3H, s, OCH₃), 3.98 (3H, s, OCH₃), 3.99 (6H, s, OCH₃), 4.12 (3H, s, OCH₃), 6.61 (1H, s, H-3), 7.00 (1H, d, *J* = 8.4 Hz, H-2'), 7.42 (1H, d, *J* = 2.0 Hz, H-5'), 7.59 (1H, dd, *J* = 2.0, 8.4 Hz, H-6'), and 12.55 (1H, s, OH). ¹H NMR (CDCl₃) spectra of 5-Ac-Nob: δ 2.45 (3H, s, (CO)CH₃), 3.86 (3H, s, OCH₃), 3.93 (3H, s, OCH₃), 3.95 (3H, s, OCH₃), 4.03 (3H, s, OCH₃), 4.08 (3H, s, OCH₃), 6.52 (1H, s, H-3),

6.96 (1H, d, *J* = 8.5 Hz, H-2'), 7.36 (1H, d, *J* = 2.1 Hz, H-5'), and 7.52 (1H, dd, *J* = 2.1, 8.5 Hz, H-6') (Supplementary Figures 3–6). The structures of 5-OH-Nob and 5-Ac-Nob are given in Figure 1.

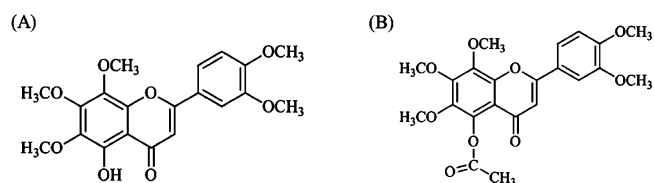


Figure 1. Chemical structures of (A) 5-OH-Nob and (B) 5-Ac-Nob.

Cell Culture and Cell Differentiation. Mouse 3T3-L1 preadipocytes purchased from the American Type Culture Collection (Rockville, MD, USA) were grown in DMEM supplemented with 2 mM glutamine (Gibco BRL), 1% penicillin/streptomycin (10000 units penicillin/mL and 10 mg streptomycin/mL), and 10% FCS in a 10 cm dish (Nunc Thermo, Waltham, MA, USA) at 37 °C under a humidified atmosphere containing 5% CO₂. After incubation with differentiation medium (DM) containing insulin, IBMX, DEX, and rosiglitazone for 8 days, 3T3-L1 preadipocytes transformed to mature adipocytes. The cells were seeded into a 96-well (2.5 × 10⁴/mL) plate or a 10 cm dish and cultured as described above. After 2 days, the cell medium was removed and replaced by 10% FBS DMEM. When the cells were confluent, defined as day 0, the cells were incubated in DM containing 5 μ g/mL insulin, 0.5 mM IBMX, 1 μ M DEX, and 2 μ M rosiglitazone in the DMEM supplemented with 10% FBS for 48 h. After 2 days, the medium was removed and the cells were incubated in the DMEM containing 10% FBS and 5 μ g/mL insulin for another 2 days, defined as day 2. Starting at day 4, the cells were incubated in DMEM containing 10% FBS, and the medium was changed every 2 days until day 8 as the DM positive [DM (+)] group. Following this protocol, different concentrations of 5-OH-Nob and 5-Ac-Nob were additionally added in the cell for another 2 days from day 0 to day 8 in the cell. The control group cells were not cultured with insulin, IBMX, DEX, and rosiglitazone from the beginning to the end of the experiment as the DM negative [DM (-)] group.

Cell Viability. The cell viability was determined by the CytoTox 96 Non-Radioactive Cytotoxicity Assay (Promega Co., San Luis Obispo, CA, USA). The 3T3-L1 preadipocytes were treated with different concentrations of 5-OH-Nob and 5-Ac-Nob in the DMEM with 10% FCS for 48 h, and then the cell viability was determined by lactate dehydrogenase (LDH) assay. LDH is a stable cytosolic enzyme. When cell membranes are damaged, LDH will leak out into the medium.¹⁸ Briefly, 50 μ L of cell supernatant was transferred to a 96-well plate and 50 μ L of reconstituted substrate mix was added and incubated for 30 min at room temperature. To each well was added 50 μ L of stop solution prior to determination of the wavelength absorbance at 490 nm. Maximum LDH release was cell treated with lysis buffer to determine the maximum LDH in cells. The percentage of cell death was calculated according to the equation

$$100\% - \% \text{ cytotoxicity} = \text{exptl LDH release} / \text{max LDH release}$$

Cell Cycle Analysis. 3T3-L1 cells were cultured in a 24-well plate followed by the cell differentiation procedure. The cells were harvested at 24 h after day 2 by trypsinization and fixed by the addition of 800 μ L of 100% ice-cold ethanol. Cells were stored at -20 °C until analysis. Before analysis by Beckman Coulter FC500 flow cytometry (Indianapolis, IN, USA), the cells were washed with PBS and centrifuged at 400g for 5 min. After centrifugation, the cells were suspended in a 500 μ L propidium iodide solution (0.2 mg/mL propidium iodide, 0.5% Triton X-100 in PBS, and 0.5 mg/mL RNase) and incubated at 37 °C for 30 min. Fluorescence intensity was quantified by flow cytometry.

Oil Red O Staining. Lipid accumulation of the 3T3-L1 cells at day 8 was determined by staining with Oil Red O. The cells were washed twice with PBS and then fixed with 10% formalin at 4 °C overnight. The Oil Red O stock solution was diluted with isopropanol (5 mg/mL) and subsequently filtered through a 0.22 μ m MCE filter. The cells were stained with Oil Red O solution diluted with distilled water for 5 min at

room temperature. After three washings with PBS, cell lipids were extracted by isopropanol and the absorbance was quantified at 510 nm wavelength.

Animal Experiments. Male C57BL/6J mice were purchased from the BioLASCO Experimental Animal Center (Taiwan Co., Ltd., Taipei, Taiwan) at 4 weeks of age. The mice were housed in a controlled temperature of $24 \pm 2^\circ\text{C}$ and 55% relative humidity with a 12 h light/dark cycle, and the mice had free access to water and food. After 1 week of acclimation, the animals were randomly divided into four groups as follows: control diet (control, 15% of calories from fat), high-fat diet (HFD; 45% of calories from fat (19.6 g of lard, 2 g of soybean oil, and 0.5% cholesterol per 100 g in the normal diet)), oral gavage at a dose of 25 mg/kg of 5-Ac-Nob with HFD as a LAN group, and oral gavage of 50 mg/kg 5-Ac-Nob with HFD as a HAN group for 13 weeks. Each group contained eight mice. The experimental diets were modified from the LabDiet 5001 standard diet (LabDiet, St. Louis, MO, USA); the nutritional composition of the food is listed in [Supplementary Table 1](#). The food intake was measured every day, and the body weight was recorded every week for 13 weeks. At the end of the study, all of the animals were fasted overnight and then sacrificed by CO_2 anesthesia. Blood samples were collected from the heart for biochemical analysis. Liver, spleen, kidney, and intra-abdominal fat (perigonadal, retroperitoneal, and mesenteric fat) were collected and weighed. The tissue samples were stored at -80°C before analysis.

Biochemical Analysis and Hepatic TG Level. Plasma samples were separated by centrifugation at 857g for 10 min at 4°C and stored at -80°C until analysis. Plasma levels of total plasma TG, cholesterol, aspartate aminotransferase (AST), and alanine aminotransferase (ALT) were measured by a commercial assay kit. Plasma samples were spotted onto separate Fujifilm Dri-Chem slides (Fujifilm, Kanagawa, Japan), and biochemical parameters were determined by a Fujifilm Dri-Chem 3500s blood biochemistry analyzer (Fujifilm) according to the manufacturer's protocol. Liver TG levels were measured using a commercial kit (Cayman Chemical Co., Ann Arbor, MI, USA). Extraction of hepatic lipid extraction followed our previous study¹⁹ from homogenization of liver tissue in 5% Triton X-100 solution and the heated homogenates at 80°C for 5–10 min to solubilize the TGs. The supernatant was collected after centrifugation at 10000g for 10 min, and the TG levels were determined according to the manufacturer's protocol.

Histological Analysis of Adipose Tissue. The method of determination of adipocyte size followed our previous study.¹⁹ Perigonadal fat was fixed in 10% formalin for 24 h and then dehydrated with a sequence of ethanol solutions and embedded in paraffin. Tissue sections (5–6 μm) were cut and stained with hematoxylin and eosin (H&E). Images were taken by an Olympus microscope under 200 \times magnification, and adipocyte size was determined by Olympus CellSens Standard.

Western Blotting. 3T3-L1 cells were harvested at day 8. Liver tissues were collected at the end of the animal experiment. Liver tissue and cell proteins were extracted by the addition of a lysis buffer (50 mM Tris-HCl, pH 7.4; 1 mM NaF; 150 mM NaCl; 1 mM EGTA; 1 mM phenylmethanesulfonyl fluoride; 1% NP-40; and 10 $\mu\text{g}/\text{mL}$ leupeptin) on ice for 1 h and then centrifuged at 10000g for 30 min at 4°C . Quantification of cell protein was carried out using a Bio-Rad Protein Assay (Bio-Rad Laboratories, Munich, Germany). A total of 25 μg of protein was mixed with 5 \times sample buffer and incubated at 100°C for 10 min. The cell protein was subjected to 10% sodium dodecyl sulfate–polyacrylamide gel electrophoresis (SDS-PAGE). After 3 h, the SDS-PAGE was transferred on the PVDF membrane (Millipore Corp., Bedford, MA, USA) with transfer buffer containing 25 mM Tris-HCl (pH 8.9), 192 mM glycine, and 20% methanol. The membranes were put in the blocking solution containing 20 mM Tris-HCl buffer with 1% of bovine serum albumin at room temperature for 1 h, and then primary antibodies including AMPK, pAMPK, LKB1, pLKB1, FAS, and β -actin (Cell Signaling Technology) were applied. The membranes were washed three times with PBST buffer for 10 min and then incubated with 1:5000 dilution of the horseradish peroxidase (HRP)-conjugated secondary antibody (Jackson ImmunoResearch, West Grove, PA, USA) and washed three times with PBST buffer. The transferred proteins were

Table 1. Effects of 5-OH-Nob and 5-Ac-Nob on Cell Viability in 3T3-L1 Cells^a

group	5-OH-Nob	5-Ac-Nob
control	87.42 \pm 1.51a	87.42 \pm 1.51a
2.5 μM	87.58 \pm 13.64a	91.98 \pm 13.45a
5 μM	84.54 \pm 15.55a	89.80 \pm 15.25a
10 μM	87.45 \pm 14.11a	83.78 \pm 15.37a
20 μM	84.82 \pm 17.78a	87.73 \pm 11.72a

^aThe 3T3-L1 cells were treated with 5-OH-Nob and 5-Ac-Nob for 48 h. The viability of 3T3-L1 cells was determined by the LDH assay. Data are expressed as the mean \pm SD ($n = 3$) and were statistically analyzed using a one-way ANOVA followed by Duncan's multiple-range test. Different letters (a, b) represent significant differences among treatments when $p < 0.05$.

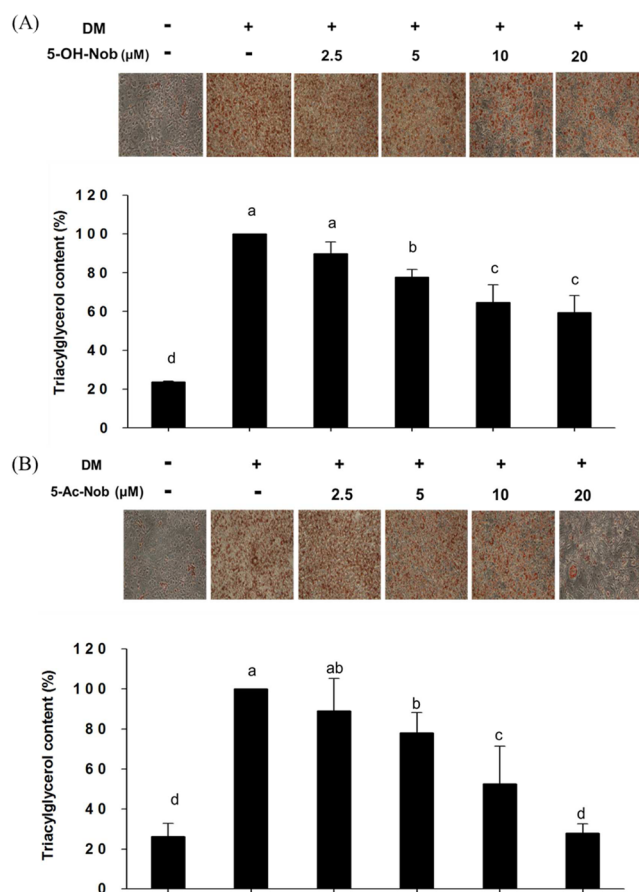


Figure 2. Effects of different concentrations of (A) 5-OH-Nob and (B) 5-Ac-Nob on triacylglycerol content in the 3T3-L1 preadipocyte model. DM (–), without differentiation medium; DM (+), with differentiation medium containing insulin, IBMX, DEX, and rosiglitazone. The cells were treated with different concentrations of 5-OH-Nob and 5-Ac-Nob for 8 days and then dyed with Oil Red O to evaluate triacylglycerol content in the cells. The cells were photographed under 200 \times magnification. Data are expressed as the mean \pm SD ($n = 3$) and were statistically analyzed using a one-way ANOVA followed by Duncan's multiple-range test. Different letters (a–d) represent significant differences among groups, $p < 0.05$.

visualized with an enhanced chemiluminescence detection kit (ECL) (Millipore Corp., Bedford, MA, USA).

Statistical Analysis. Data are presented as the mean \pm SD and analyzed by one-way analysis of variance (ANOVA) and Duncan's multiple-comparison tests (SAS Institute Inc., Cary, NC, USA). $p < 0.05$ represents a significant difference among treatment groups.

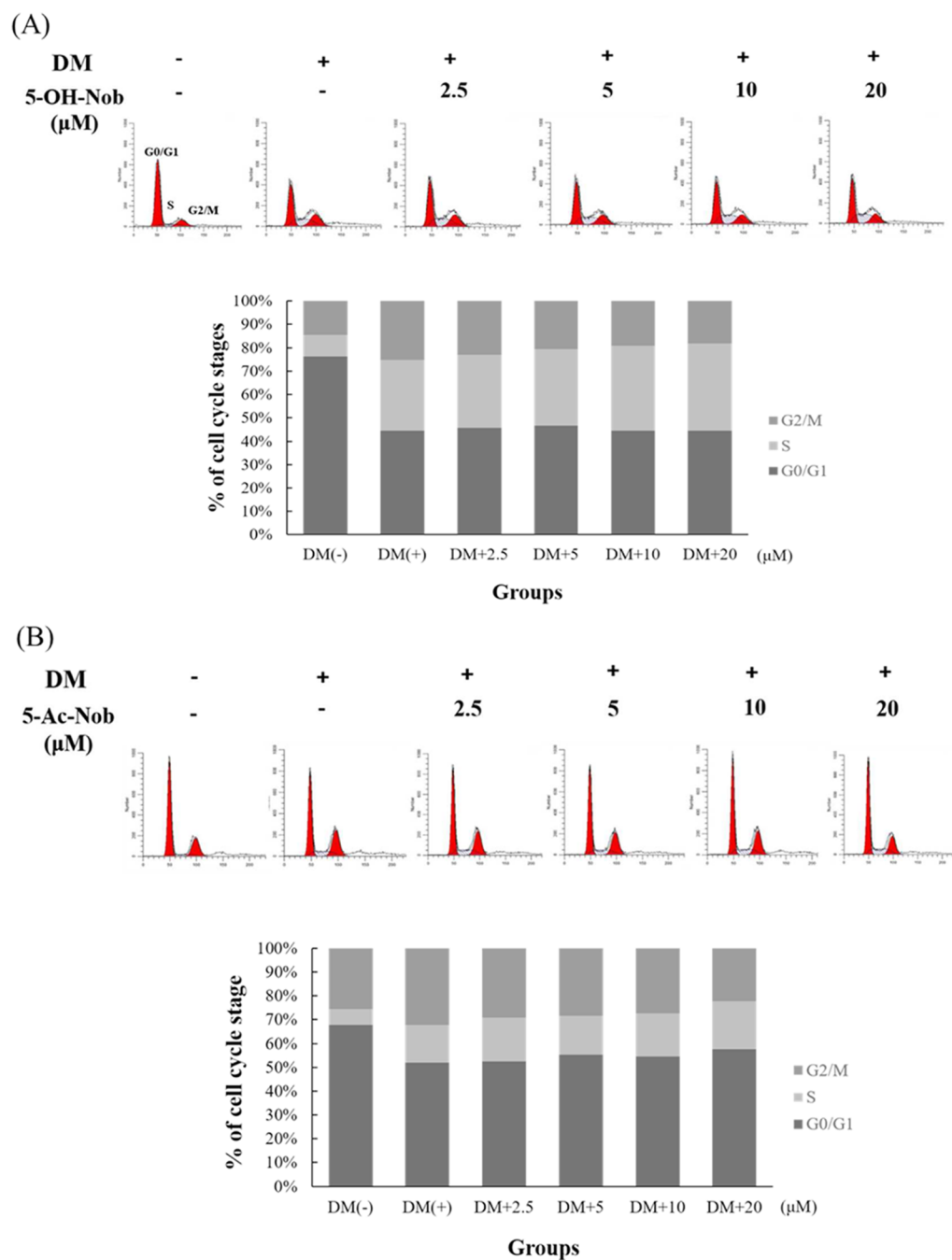


Figure 3. Effects of different concentrations of (A) 5-OH-Nob and (B) 5-Ac-Nob on the cell cycle in 3T3-L1 preadipocytes. DM (-), without the differentiation medium; DM (+), with differentiation medium containing insulin, IBMX, DEX, and rosiglitazone.

RESULTS

Effects of 5-OH-Nob and 5-Ac-Nob on Cell Viability and Lipid Accumulation in 3T3-L1 Preadipocytes. We used a CytoTox 96 Non-Radioactive Cytotoxicity Assay kit to determine the LDH levels, which are a measure of cell viability. The 3T3-L1 preadipocyte cells were treated with 2.5, 5, 10, and 20 μM 5-OH-Nob and 5-Ac-Nob for 48 h. Our results showed that treatment with 5-OH-Nob and 5-Ac-Nob at various concentrations did not significantly alter cell viabilities compared to the control group, indicating that both 5-OH-Nob and 5-Ac-Nob did not cause cytotoxicity in 3T3-L1 preadipocytes (Table 1). We further investigated their effects during adipogenesis and determined the TG content in 3T3-L1 preadipocytes.

When the cells were treated with 2.5, 5, 10, and 20 μM 5-OH-Nob and 5-Ac-Nob during the differentiation process, we found that both 5-OH-Nob and 5-Ac-Nob significantly decreased TG content in the mature cells in dose-dependent manners. After treatment with 20 μM 5-OH-Nob (Figure 2A) and 5-Ac-Nob (Figure 2B), the TG levels decreased by 35 and 70%, respectively, suggesting that 5-Ac-Nob is twice as potent as 5-OH-Nob in decreasing lipid accumulation in 3T3-L1 adipocytes.

Effect of 5-OH-Nob and 5-Ac-Nob on the Cell Cycle of 3T3-L1 Preadipocytes. To evaluate the antiadipogenic effects of 5-OH-Nob and 5-Ac-Nob, we further determined whether 5-OH-Nob and 5-Ac-Nob could affect the growth of 3T3-L1 preadipocytes by analyzing the cell cycle. The results showed that

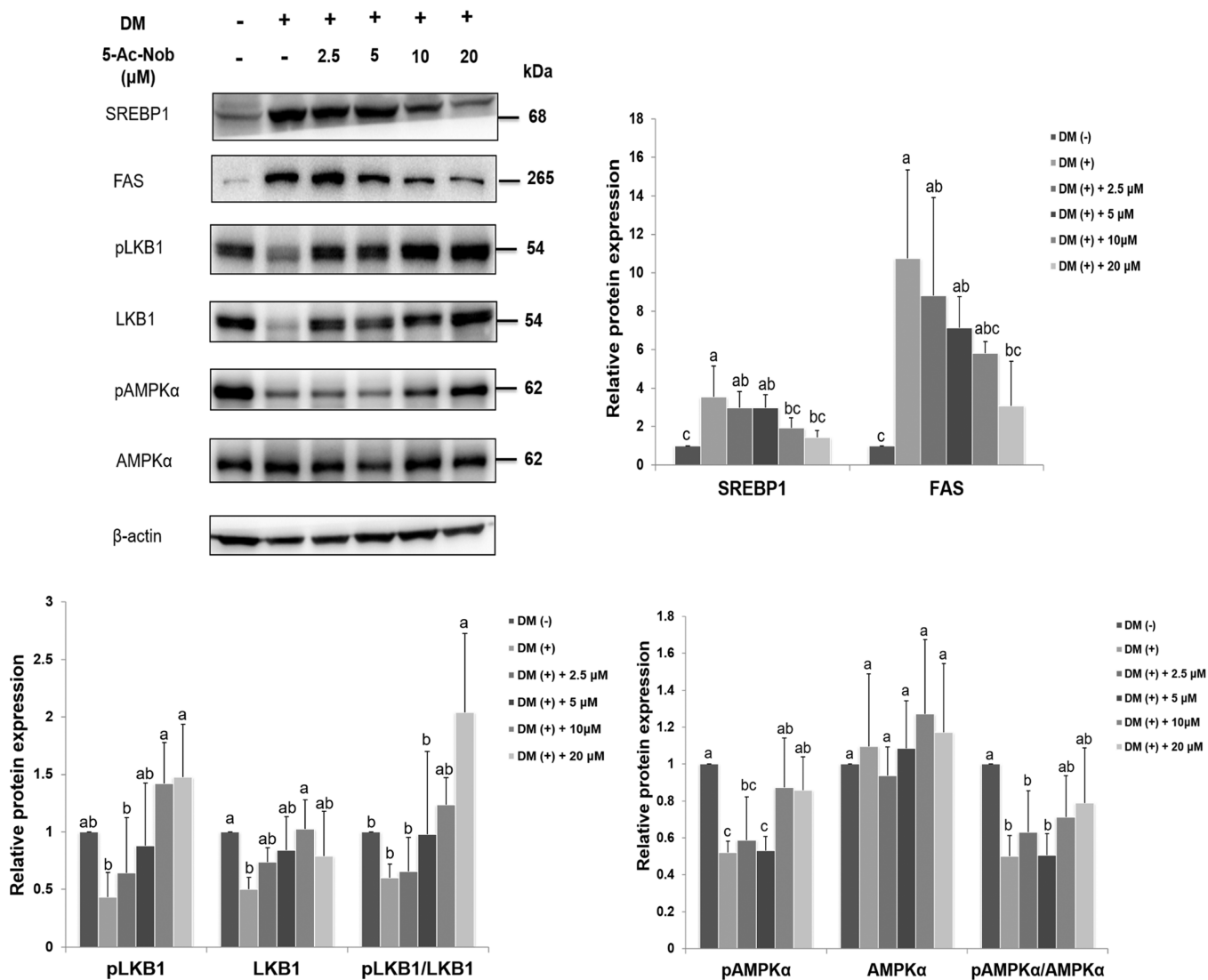


Figure 4. Effects of 5-Ac-Nob on LKB1, AMPK, SREBP-1, and FAS protein expression in 3T3-L1 adipocytes. Protein expression levels were determined relative to actin in three independent experiment. Data are expressed as the mean \pm SD ($n = 3$) and were statistically analyzed using a one-way ANOVA and Duncan's test. Different letters (a–c) represent significant differences among groups when $p < 0.05$.

67–76% of the cells (10000 cells) were in G0/G1 phase and 7–9% in S phase in the DM (–) group, whereas 45–52% of the cells were in G0/G1 phase and 16–30% of the cells were in S phase in the DM (+) group. The cells in the DM (+) group showed cell cycle progression. After treatment with 2.5, 5, 10, and 20 μ M 5-OH-Nob and 5-Ac-Nob for 24 h, the results of cell cycle analysis were similar to the DM (+) group, indicating that both 5-OH-Nob and 5-Ac-Nob did not induce 3T3-L1 cell apoptosis or cell cycle arrest. The 5-OH-Nob and 5-Ac-Nob treatments did not affect cell growth in the early stage of cell differentiation (Figure 3).

Effect of 5-Ac-Nob on the LKB1-AMPK Signaling Pathway in 3T3-L1 Preadipocytes. The 5-Ac-Nob treatment did not affect the 3T3-L1 preadipocyte growth; therefore, its reduction of TG levels may occur in the late stage of 3T3-L1 preadipocyte differentiation. Because 5-Ac-Nob showed a stronger TG decrease than 5-OH-Nob, we further examined the effects of 5-Ac-Nob on the lipid synthesis-related protein expression in the late stage of cell differentiation. We found that the expression of SREBP-1, phosphorylated ACC (pACC), and FAS protein in the DM (+) group was higher than in the DM (–) group.

Treatment with 5-Ac-Nob effectively decreased SREBP-1 and FAS protein levels in the late stage of cell differentiation (Figure 4) but did not increase pACC protein expression (Supplementary Figure 7). We also found that cells in the DM (+) group had lower levels of LKB1, pLKB1, and pAMPK α than the DM (–) group. Additionally, 5-Ac-Nob increased LKB1, phosphorylated LKB1 (pLKB1), and phosphorylated AMPK α (pAMPK α) protein expression compared to the DM (+) group. Taken together, our results indicate that 5-Ac-Nob could increase pLKB1 and pAMPK α protein levels and subsequently affect lipid synthesis-related protein expression in the late stage of cell differentiation (Figure 4).

Effect of 5-Ac-Nob on Body Weight and Intra-abdominal Fat Weight in the High Fat Diet-Induced Obese Animals. As described above, we found that 5-Ac-Nob potentially inhibited lipid accumulation in 3T3-L1 adipocytes better than 5-OH-Nob, and we further investigated its effects on lipid accumulation in vivo. The mice were fed a diet with 45% of calories from fat for 13 weeks and administered 25 and 50 mg/kg 5-Ac-Nob by oral gavage. After 13 weeks, the body weight of the HFD group was 29.6 ± 2.5 g, significantly higher than that of the

Table 2. Effects of 5-Ac-Nob on Body Weight, Food Intake, and Organ Weight^a

	control	HFD ^b	HFD+LAN ^c	HFD+HAN ^d
initial wt (g)	18.4 ± 0.8a	18.9 ± 0.8a	18.2 ± 0.7a	18.6 ± 0.6a
final wt (g)	25.5 ± 1.1c	29.6 ± 2.5a	27.0 ± 1.0bc	27.5 ± 0.8b
wt gain (g)	7.1 ± 1.1c	10.6 ± 1.9a	8.8 ± 0.8b	8.9 ± 1.1b
food intake (g/mouse/day)	4.4 ± 0.9a	3.4 ± 0.5bc	3.0 ± 0.3c	3.5 ± 0.4b
food efficiency ratio ^e	0.13 ± 0.07b	0.23 ± 0.06a	0.22 ± 0.06a	0.21 ± 0.05a
liver wt (g)	1.25 ± 0.05ab	1.25 ± 0.05ab	1.26 ± 0.06a	1.20 ± 0.04b
kidney wt (g)	0.42 ± 0.01a	0.42 ± 0.01a	0.41 ± 0.02a	0.42 ± 0.02a
spleen wt (g)	0.07 ± 0.01a	0.06 ± 0.01a	0.06 ± 0.01a	0.06 ± 0.01a

^aData are expressed as the mean ± SD ($n = 8$) and were statistically analyzed using one-way ANOVA followed by Duncan's multiple-range test. Different letters (a–c) represent significant differences among treatments when $p < 0.05$. ^bHFD, high-fat diet. ^cLAN, 25 mg/kg of 5-Ac-Nob. ^dHAN, 50 mg/kg of 5-Ac-Nob. ^eFood efficiency ratio gain of body weight (g)/food intake (g).

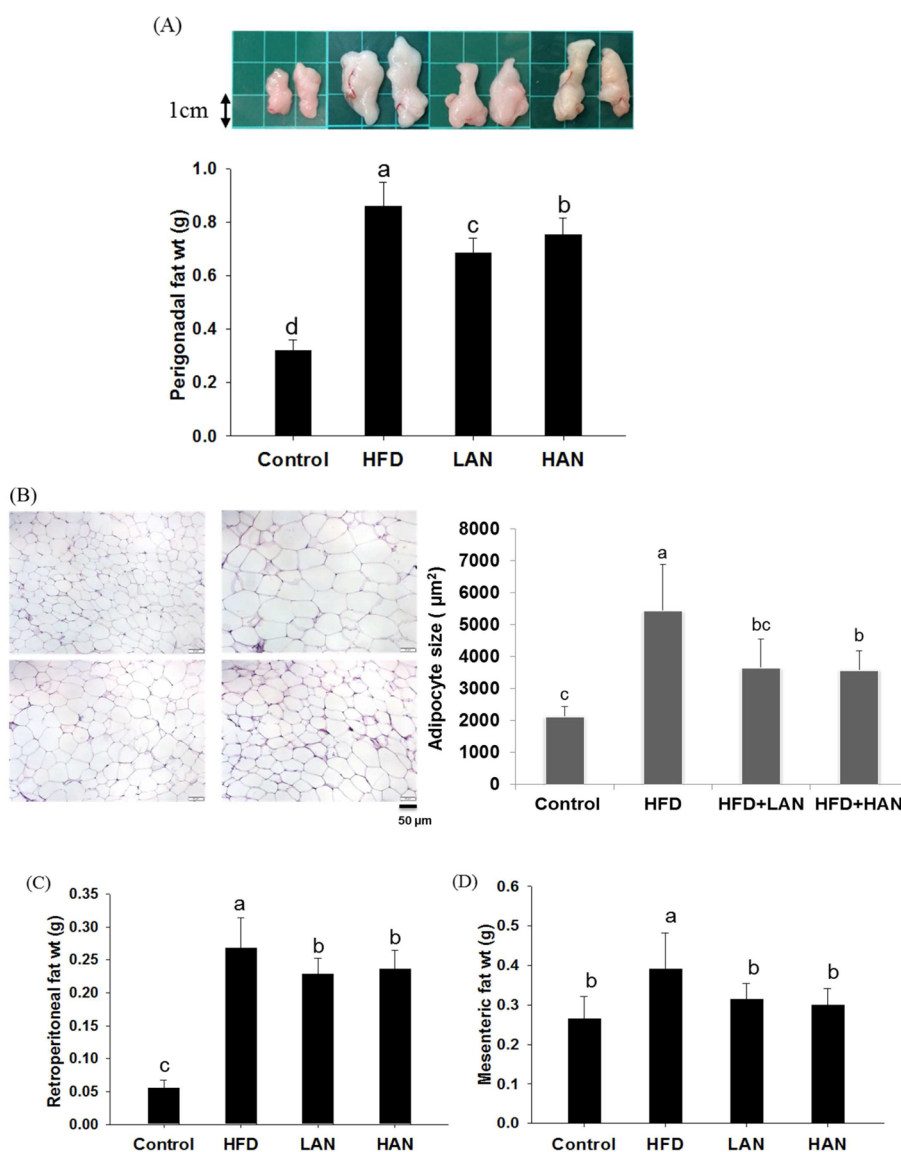


Figure 5. Effects of 5-Ac-Nob on intra-abdominal fat weight, (A) perigonadal fat; (B) histological analysis of perigonadal fat by H&E staining (200× magnification) and adipocyte size (µm²); (C) retroperitoneal fat and (D) mesenteric fat in the HFD-induced obesity animal model. Data are expressed as the mean ± SD ($n = 3$) and were statistically analyzed using one-way ANOVA and Duncan's test. Different letters (a–d) represent significant differences among groups when $p < 0.05$. HFD, high-fat diet; LAN, 25 mg/kg of 5-Ac-Nob; HAN, 50 mg/kg of 5-Ac-Nob.

control group (25.5 ± 1.1 g). The body weights of the LAN and HAN groups were 27 ± 1.0 and 27.5 ± 0.8 g, respectively, lower than that of the HFD group (Table 2). During the experiment, food intake was recorded daily, and the results showed that the

control group had a higher food intake than the HFD, LAN, and HAN groups, whereas there were no significant differences in food intake among the HFD, LAN, and HAN groups. HFD had higher weight gain than the LAN and HAN groups at the same

Table 3. Effects of 5-Ac-Nob on Serum Biochemical Parameters^a

	control	HFD ^b	HFD+LAN ^c	HFD+HAN ^d
TG (mg/dL)	74.6 ± 5.3b	97.1 ± 13.8a	94.6 ± 13.2a	82.1 ± 7.1b
T-cholesterol (mg/dL)	63.9 ± 4.8c	134.4 ± 8.1a	132.8 ± 7.3a	117.4 ± 11.0b
AST (U/L)	116.6 ± 29.3a	110.6 ± 17.4a	124.8 ± 38.3a	106.3 ± 26.3a
ALT (U/L)	41.4 ± 3.0a	27.3 ± 2.2b	38.8 ± 18.3a	27.6 ± 1.9b

^aData are expressed as the mean ± SD ($n = 8$) and were statistically analyzed using one-way ANOVA and Duncan's test. Different letters (a–c) represent significant differences among treatments, $p < 0.05$. ^bHFD, high-fat diet. ^cLAN, 25 mg/kg 5-Ac-Nob; ^dHAN, 50 mg/kg 5-Ac-Nob.

food efficiency ratio (Table 2). At the end of the experiment, liver, kidney, spleen, and intra-abdominal fat, including perigonadal fat, retroperitoneal fat, and mesenteric fat, were collected and weighed. The organ weights did not show significant differences among the groups (Table 2). The weight of the intra-abdominal fat and the adipocyte size of the HFD group were significantly higher than those of the control, LAN, and HAN groups (Figure 5).

Effects of 5-Ac-Nob on Serum Biochemistry and Hepatic Triacylglycerol Content in the High Fat Diet-Induced Obese Animal Model. As shown in Table 3, the serum AST levels did not show significant differences among the four groups tested. The HFD and HAN groups had lower ALT levels than the control and LAN groups. The total serum cholesterol level of the HAN group was 117.4 ± 11.0 mg/dL, and that of the control group was 63.9 ± 4.8 mg/dL, significantly lower than that of the HFD group (134.4 ± 8.1 mg/dL). The serum TG level of the HFD group was 97.1 ± 13.8 mg/dL, significantly higher than that of the control group (74.6 ± 5.3 mg/dL) or the HAN group (82.1 ± 7.1 mg/dL). The total serum cholesterol levels had a trend similar to that of the serum TG levels (Table 3). As shown in Figure 6, the TG levels in

the HFD group had lower pAMPK α protein levels than the control group. The HAN group showed increased pLKB1 and pAMPK α protein levels compared to the HFD group; especially the HAN group had significantly increased pAMPK α protein levels relative to the HFD group. We also found that the HFD group had lower pACC protein levels than the control group. The LAN and HAN groups had elevated pACC protein levels compared to the HFD group. The HFD group had lower SREBP-1 and FAS protein levels than the control and LAN groups. The LAN and HAN groups did not show decreased SREBP-1 and FAS protein levels (Supplementary Figure 8). These results indicate that the HAN group had decreased lipid accumulation in the liver due to increased pLKB1 and pAMPK α protein levels and increased pACC lipid synthesis-related protein expression.

DISCUSSION

Several recent studies have reported that suppressing adipogenesis in the adipocytes can help control body weight. Some plant extracts, such as raspberry ketones and PMFs and HPMFs in citrus peel extracts, were found to regulate lipid metabolism in 3T3-L1 adipocytes and high fat diet-induced obesity animal models.^{20–22} However, PMFs and HPMFs have poor aqueous solubility, which leads to low oral bioavailability.^{11,14} In this study, we used the prodrug concept and successfully prepared an acetylated derivative of 5-OH-Nob that can release the active parent molecules by metabolic transformation in vivo to enhance its oral bioavailability.¹⁵ Our current data demonstrated that a 5-OH-Nob derivative, 5-Ac-Nob, decreased TG content to a greater extent in the 3T3-L1 adipocytes than its parent compound. In addition, we also found that 5-Ac-Nob effectively decreased lipid accumulation in the high fat diet-induced obese animal model. A previous study showed that nobiletin decreased TG accumulation by 80% at a concentration of 100 μ M in the 3T3-L1 cells.²³ In this study, we found that both 5-OH-Nob and 5-Ac-Nob effectively decreased TG content at concentrations of 5, 10, and 20 μ M without any cytotoxicity (Figure 2). Adipogenesis is a complicated process that includes early phase growth arrest, mitotic clonal expansion, and late-phase lipogenesis-related enzyme expression from preadipocytes to mature adipocytes.²⁴ The antiadipogenic activity of HPMFs resulted from blocking the early phase cell cycle progression and causing cell cycle arrest in G0/G1 phase.²¹ In this study, when the cells were treated with 5-OH-Nob and 5-Ac-Nob, they still underwent cell cycle progression to S phase, and compared to the DM (–) group, the cells stayed in G0/G1 phase (Figures 4 and 5). These results suggest that the antiadipogenic effects of 5-OH-Nob and 5-Ac-Nob may affect the late stage of adipogenesis. (Table 1; Figures 4 and 5). Our results showed that 5-Ac-Nob inhibited TG content to a greater extent than 5-OH-Nob in 3T3-L1 adipocytes. We further investigated the effects of 5-Ac-Nob in an HFD-induced obesity animal model. Here, we found that 50 mg/kg (HAN group) 5-Ac-Nob significantly reduced the

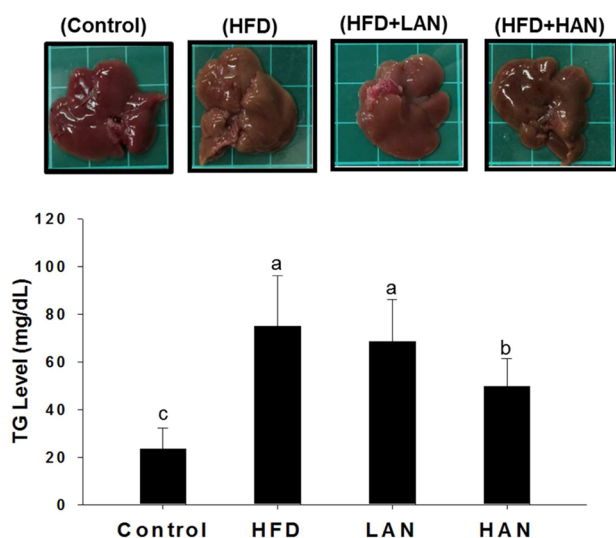


Figure 6. Effects of 5-Ac-Nob on TG levels in the mouse liver. Data are expressed as the mean ± SD ($n = 8$) and were statistically analyzed using one-way ANOVA and Duncan's test. Different letters (a–c) represent significant differences among treatments when $p < 0.05$. HFD, high-fat diet; LAN, 25 mg/kg 5-Ac-Nob; HAN, 50 mg/kg 5-Ac-Nob.

the liver were 23.5 ± 8.7 , 74.8 ± 21.4 , 68.5 ± 17.5 , and 49.6 ± 11.9 mg/dL in the control, HFD, LAN, and HAN groups, respectively. Therefore, the high dose of 5-Ac-Nob substantially decreased the TG levels in both the serum and liver.

Effect of 5-Ac-Nob on the LKB1-AMPK Signaling Pathway in the Liver. As shown in Figure 7, we found that

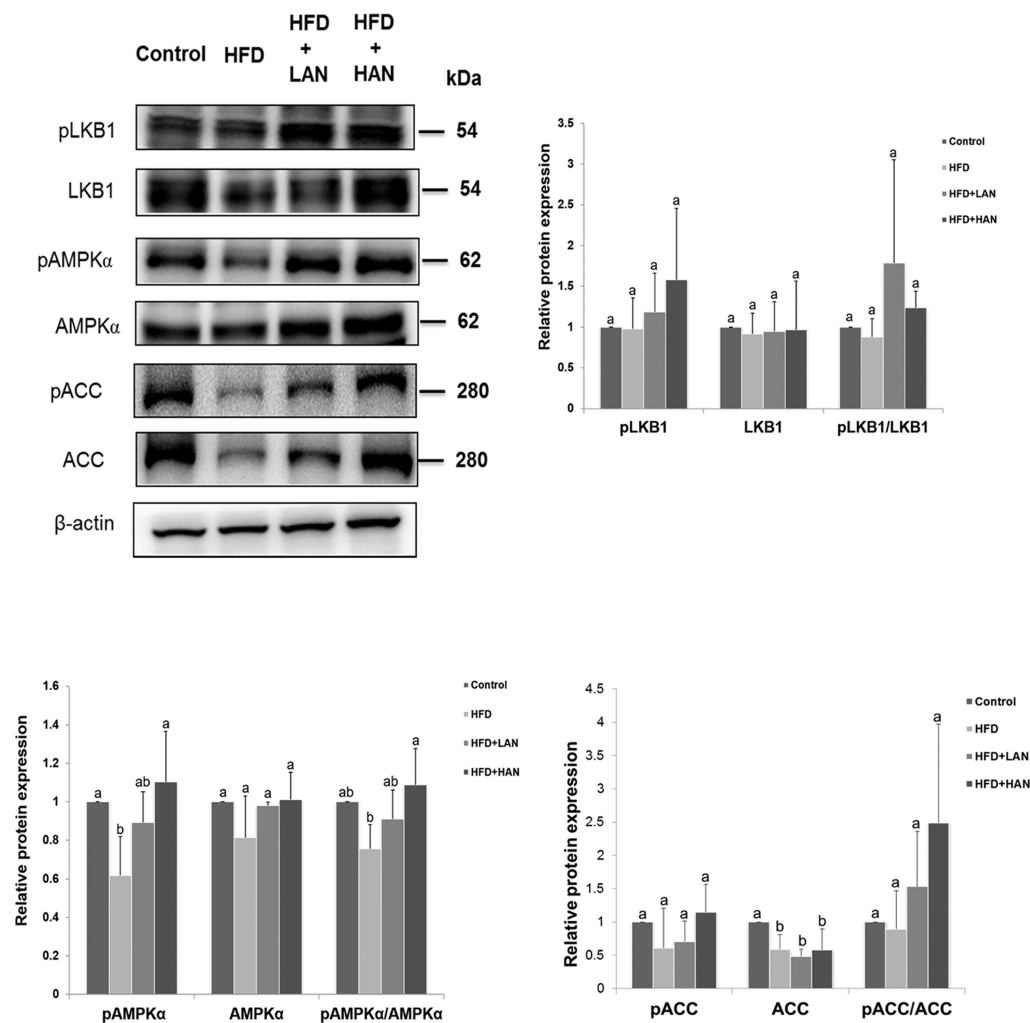


Figure 7. Effects of 5-Ac-Nob on the phosphorylation of LKB1, AMPK α , and ACC and the protein levels of LKB1, AMPK α , and ACC. Lipid accumulation was inhibited via activation of the LKB1-AMPK pathway and pACC protein levels in an HFD-induced obesity animal model. Protein expression was determined relative to actin in three independent experiments. Data are expressed as the mean \pm SD and were statistically analyzed using one-way ANOVA and Duncan's test. Different letters (a, b) represent significant differences among groups when $p < 0.05$. HFD, high-fat diet; LAN, 25 mg/kg 5-Ac-Nob; HAN, 50 mg/kg 5-Ac-Nob.

body weight, intra-abdominal adipose tissue (retroperitoneal, perirenal, mesenteric, and perigonadal are intra-abdominal fats in mice) weight, plasma TGs, and total cholesterol compared to the HFD group (Figure 5; Tables 2 and 3). The liver is the major organ that regulates glucose and lipid metabolism, controlling energy balance and body weight.²⁵ Excess fat around the liver (intra-abdominal adipose) can be more easily transported into the liver by portal circulation as free fatty acids, which would induce TG synthesis in the liver.²⁶ In our current study, we found that 50 mg/kg 5-Ac-Nob significantly decreased liver TG levels (Figure 6).

We demonstrated that 5-Ac-Nob could decrease TGs in both the 3T3-L1 cells and high fat diet-induced obese mice. SREBPs are transcription factors that are involved in cellular lipogenesis and lipid homeostasis by regulating cholesterol, fatty acids, TGs, and phospholipid synthesis-related enzyme expression.^{3,7} Generally, the activation of SREBPs involves a two-step proteolytic cascade. In the first step, SREBP is cleaved from the SREBP/SREBP cleavage-activating protein (SCAP) complex (125 kDa) at the endoplasmic reticulum membrane, and in the second step, cleavage releases the mature SREBPs (68 kDa) to the nucleus to activate transcriptional activity.²⁷ Here, we found that 5-Ac-Nob

decreased the nuclear form of the SREBP-1 protein (68 kDa) in 3T3-L1 preadipocytes, but SREBP-1 protein expression was not decreased in the liver. Lipogenesis is a complicated process, and several crucial enzymes, such as ACC and FAS, are involved.²⁸ We found that 5-Ac-Nob decreased FAS protein levels, whereas pACC protein levels in 3T3-L1 cells were not increased. Interestingly, we have observed that 5-Ac-Nob increased the expression of the pACC protein, a crucial enzyme involved in the initial step of lipogenesis²⁸ in the liver. However, 5-Ac-Nob did not decrease the SREBP-1 and FAS protein expressions compared to the HFD group in the liver. AMPK plays a key role in energy homeostasis, and it can inhibit fatty acid synthesis by directly phosphorylating ACC or FAS or inhibiting the proteolytic cleavage of SREBP-1.^{29,30} LKB1 can up-regulate AMPK by phosphorylating a threonine residue at position 172 in an α catalytic subunit.³¹ Here, we found that 5-Ac-Nob increased pAMPK α protein expression in 3T3-L1 cells and in the liver.

In conclusion, we found that both 5-OH-Nob and 5-Ac-Nob decreased TG levels in 3T3-L1 cells effectively, but 5-Ac-Nob was more potent. Hence, we used 5-Ac-Nob to further evaluate the antiobesity effects in an obese animal model induced by a high-fat diet. We observed that 5-Ac-Nob not only suppressed

lipid accumulation to a greater extent than 5-OH-Nob in the 3T3-L1 cell model but also decreased body weight, alleviated hyperlipidemia, and decreased liver TG content in the high fat diet-induced obese mice. The 5-Ac-Nob treatment suppressed lipid accumulation by activating the LKB1-AMPK pathway and subsequently affected lipogenesis-related protein expression in the cells and livers and the related transcriptional factor SREBP-1 in cells (Figure 8). Thus, on the basis of the *in vivo* results

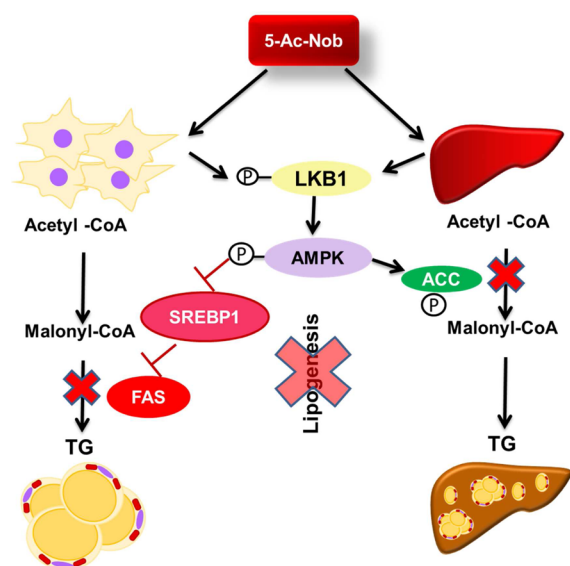


Figure 8. Possible mechanisms of 5-Ac-Nob for suppressing lipid accumulation in the 3T3-L1 preadipocytes and mouse liver tissue.

obtained from our current study, we suggest that 5-Ac-Nob may become a potential candidate for controlling obesity or delaying the onset of fatty liver disease. Additionally, this research provides more evidence that acetylation of hydroxylated nobiletin is an effective method to develop a prodrug with a greater efficacy in suppressing lipid accumulation than 5-OH-Nob, its naturally occurring parent compound from citrus peels. Future studies should clarify the metabolism of 5-Ac-Nob and its relationship with 5-OH-Nob *in vivo*.

■ ASSOCIATED CONTENT

Supporting Information

The Supporting Information is available free of charge on the ACS Publications website at DOI: 10.1021/acs.jafc.6b00706.

Figure S1: LC-MS of 5-OH-Nob. LC-MS was performed by a Thermo Scientific linear ion trap mass spectrometer (LXQTM) in positive ionization mode (Thermo Scientific, Waltham, MA, USA). Figure S2: LC-MS of 5-Ac-Nob. LC-MS was performed by a Thermo Scientific linear ion trap mass spectrometer (LXQTM) in positive ionization mode. Figure S3: ^1H NMR of 5-OH-Nob. NMR spectra were recorded on a Bruker AVIII 500 MHz FT-NMR (Bruker, Rheinstetten, Germany) in CDCl_3 . Figure S4: ^{13}C NMR of 5-OH-Nob. NMR spectra were recorded on a Bruker AVIII 500 MHz FT-NMR in CDCl_3 . Figure S5: ^1H NMR of 5-Ac-Nob. NMR spectra were recorded on a Bruker AVIII 500 MHz FT-NMR in CDCl_3 . Figure S6: ^{13}C NMR of 5-Ac-Nob. NMR spectra were recorded on a Bruker AVIII 500 MHz FT-NMR in CDCl_3 . Figure S7: Relative protein expression of pACC in 3T3-L1 adipocyte. Protein expression levels were determined

relative to actin in three independent experiment. Data are expressed as the mean \pm SD ($n = 3$) and were statistically analyzed using a one-way ANOVA and Duncan's test. Different letters (a, b) represent significant differences among groups when $p < 0.05$. Figure S8: Relative protein expression of SREBP1 and FAS in HFD-induced animal model. Protein expression levels were determined relative to actin in three independent experiment. Data are expressed as the mean \pm SD ($n = 3$) and were statistically analyzed using a one-way ANOVA and Duncan's test. Different letters (a, b) represent significant differences among groups when $p < 0.05$. Table S1: Composition of diets. The control diets were LabDiet 5001 standard diet bought from LabDiet (St. Louis, MO, USA). The HFD diet was modified from LabDiet 5001 standard diet, containing an extra 19.6 g of lard, 2 g of soybean, and 0.5 g of cholesterol in 100 g of LabDiet 5001 standard diet (PDF)

■ AUTHOR INFORMATION

Corresponding Authors

* (M.-H.P.) Phone: +886 2 33664133. Fax: +886-2-3366-1771. E-mail: mhpan@ntu.edu.tw.

* (G.-J.W.) Phone: +886-3-341-2500, ext. 2512. Fax: +886-3-270-5904. E-mail: gwei@mail.knu.edu.tw.

Funding

This study was supported by the National Taiwan University NTU-104R7777; the Ministry of Science and Technology 101-2628-B-022-001-MY4, 102-2628-B-002-053-MY3; and a collaboration grant of Hubei province, China (2014BHE036).

Notes

The authors declare no competing financial interest.

■ REFERENCES

- (1) WHO. Fact sheet: obesity and overweight, 2015; <http://www.who.int/dietphysicalactivity/publications/facts/obesity/en/>.
- (2) Symonds, M. E. *Adipose Tissue Biology*; Springer Science & Business Media: Berlin, Germany, 2012.
- (3) Desvergne, B.; Michalik, L.; Wahli, W. Transcriptional regulation of metabolism. *Physiol. Rev.* **2006**, *86*, 465–514.
- (4) Blüher, M. Adipose tissue dysfunction contributes to obesity related metabolic diseases. *Best Pract. Res. Clin. Endocrinol. Metabol.* **2013**, *27*, 163–177.
- (5) Zalesin, K. C.; Franklin, B. A.; Miller, W. M.; Peterson, E. D.; McCullough, P. A. Impact of obesity on cardiovascular disease. *Med. Clin. North Am.* **2011**, *95*, 919–937.
- (6) Ali, A. T.; Hochfeld, W. E.; Myburgh, R.; Pepper, M. S. Adipocyte and adipogenesis. *Eur. J. Cell Biol.* **2013**, *92*, 229–236.
- (7) Horton, J. D.; Shimomura, I.; Ikemoto, S.; Bashmakov, Y.; Hammer, R. E. Overexpression of sterol regulatory element-binding protein-1a in mouse adipose tissue produces adipocyte hypertrophy, increased fatty acid secretion, and fatty liver. *J. Biol. Chem.* **2003**, *278*, 36652–36660.
- (8) Lage, R.; Diéguez, C.; Vidal-Puig, A.; López, M. AMPK: a metabolic gauge regulating whole-body energy homeostasis. *Trends Mol. Med.* **2008**, *14*, 539–549.
- (9) Sanders, M. J.; Grondin, P. O.; Hegarty, B. D.; Snowden, M. A.; Carling, D. Investigating the mechanism for AMP activation of the AMP-activated protein kinase cascade. *Biochem. J.* **2007**, *403*, 139–148.
- (10) Mihaylova, M. M.; Shaw, R. J. The AMPK signalling pathway coordinates cell growth, autophagy and metabolism. *Nat. Cell Biol.* **2011**, *13*, 1016–1023.
- (11) Li, S.; Pan, M. H.; Lo, C. Y.; Tan, D.; Wang, Y.; Shahidi, F.; Ho, C. T. Chemistry and health effects of polymethoxyflavones and hydroxylated polymethoxyflavones. *J. Funct. Foods* **2009**, *1*, 2–12.

(12) Miyata, Y.; Tanaka, H.; Shimada, A.; Sato, T.; Ito, A.; Yamanouchi, T.; Kosano, H. Regulation of adipocytokine secretion and adipocyte hypertrophy by polymethoxyflavonoids, nobiletin and tangeretin. *Life Sci.* **2011**, *88*, 613–618.

(13) Kanda, K.; Nishi, K.; Kadota, A.; Nishimoto, S.; Liu, M. C.; Sugahara, T. Nobiletin suppresses adipocyte differentiation of 3T3-L1 cells by an insulin and IBMX mixture induction. *Biochim. Biophys. Acta, Gen. Subj.* **2012**, *1820*, 461–468.

(14) Li, S.; Wang, H.; Guo, L.; Zhao, H.; Ho, C. T. Chemistry and bioactivity of nobiletin and its metabolites. *J. Funct. Foods* **2014**, *6*, 2–10.

(15) Rautio, J.; Kumpulainen, H.; Heimbach, T.; Oliyai, R.; Oh, D.; Järvinen, T.; Savolainen, J. Prodrugs: design and clinical applications. *Nat. Rev. Drug Discovery* **2008**, *7*, 255–270.

(16) Vane, J.; Botting, R. The mechanism of action of aspirin. *Thromb. Res.* **2003**, *110*, 255–258.

(17) Wang, J.; Duan, Y.; Zhi, D.; Li, G.; Wang, L.; Zhang, H.; Gu, L.; Ruan, H.; Zhang, K.; Liu, Q. Pro-apoptotic effects of the novel tangeretin derivate 5-acetyl-6,7,8,4'-tetramethylnortangeretin on mcf-7 breast cancer cells. *Cell Biochem. Biophys.* **2014**, *70*, 1255–1263.

(18) Korzeniewski, C.; Callewaert, D. M. An enzyme-release assay for natural cytotoxicity. *J. Immunol. Methods* **1983**, *64*, 313–320.

(19) Lai, C. S.; Liao, S. N.; Tsai, M. L.; Kalyanam, N.; Majeed, M.; Majeed, A.; Ho, C. T.; Pan, M. H. Calebin-A inhibits adipogenesis and hepatic steatosis in high-fat diet-induced obesity via activation of AMPK signaling. *Mol. Nutr. Food Res.* **2015**, *59*, 1883–1895.

(20) Park, K. S. Raspberry ketone increases both lipolysis and fatty acid oxidation in 3T3-L1 adipocytes. *Planta Med.* **2010**, *76*, 1654–1658.

(21) Lai, C. S.; Ho, M. H.; Tsai, M. L.; Li, S.; Badmaev, V.; Ho, C. T.; Pan, M. H. Suppression of adipogenesis and obesity in high-fat induced mouse model by hydroxylated polymethoxyflavones. *J. Agric. Food Chem.* **2013**, *61*, 10320–10328.

(22) Lee, Y. S.; Cha, B. Y.; Choi, S. S.; Choi, B. K.; Yonezawa, T.; Teruya, T.; Nagai, K.; Woo, J. T. Nobiletin improves obesity and insulin resistance in high-fat diet-induced obese mice. *J. Nutr. Biochem.* **2013**, *24*, 156–162.

(23) Choi, Y.; Kim, Y.; Ham, H.; Park, Y.; Jeong, H. S.; Lee, J. Nobiletin suppresses adipogenesis by regulating the expression of adipogenic transcription factors and the activation of AMP-activated protein kinase (AMPK). *J. Agric. Food Chem.* **2011**, *59*, 12843–12849.

(24) Gregoire, F. M.; Smas, C. M.; Sul, H. S. Understanding adipocyte differentiation. *Physiol. Rev.* **1998**, *78*, 783–809.

(25) Corey, K. E.; Kaplan, L. M. Obesity and liver disease: the epidemic of the twenty-first century. *Clin. Liver Dis.* **2014**, *18*, 1–18.

(26) Bjørndal, B.; Burri, L.; Staalesen, V.; Skorve, J.; Berge, R. K. Different adipose depots: their role in the development of metabolic syndrome and mitochondrial response to hypolipidemic agents. *J. Obes.* **2011**, *2011*, 490650.

(27) Weber, L. W.; Boll, M.; Stampfl, A. Maintaining cholesterol homeostasis: sterol regulatory element-binding proteins. *World J. Gastroenterol.* **2004**, *10*, 3081–3087.

(28) Lodhi, I. J.; Wei, X.; Semenkovich, C. F. Lipoexpediency: de novo lipogenesis as a metabolic signal transmitter. *Trends Endocrinol. Metab.* **2011**, *22*, 1–8.

(29) Hardie, D. AMPK: a key regulator of energy balance in the single cell and the whole organism. *Int. J. Obes.* **2008**, *32*, S7–S12.

(30) Li, Y.; Xu, S.; Mihaylova, M. M.; Zheng, B.; Hou, X.; Jiang, B.; Park, O.; Luo, Z.; Lefai, E.; Shyy, J. Y.-J. AMPK phosphorylates and inhibits SREBP activity to attenuate hepatic steatosis and atherosclerosis in diet-induced insulin-resistant mice. *Cell Metab.* **2011**, *13*, 376–388.

(31) Shaw, R. J.; Kosmatka, M.; Bardeesy, N.; Hurley, R. L.; Witters, L. A.; DePinho, R. A.; Cantley, L. C. The tumor suppressor LKB1 kinase directly activates AMP-activated kinase and regulates apoptosis in response to energy stress. *Proc. Natl. Acad. Sci. U.S.A.* **2004**, *101*, 3329–3335.